

# Providing Guaranteed Performances for an Enhanced Cruise Control Using Robust LPV Method

**Balázs Németh**

Institute for Computer Science and Control (SZTAKI), Eötvös Loránd Research Network (ELKH), Kende u. 13-17, H-1111 Budapest, Hungary  
e-mail: balazs.nemeth@sztaki.hu

---

*Abstract: The paper proposes the design of an enhanced cruise control system for automated vehicles. The control strategy has three components, such as a predictive optimal control, a robust Linear Parameter-Varying (LPV) control and an optimization-based supervisor. In the design process of the control, primary performances (safety and speed limitation requirements) and secondary performances (economy and traveling time criteria) are considered. These performances are guaranteed through the different control components. The enhanced cruise control is able to provide solution to complex cruise control scenarios with a guaranteed performance level. The effectiveness of the method is illustrated through various simulation examples, in which the loss of the performance level is avoided by the proposed control.*

---

*Keywords: automated vehicle cruise control; LPV control design; performance specifications*

---

## 1 Introduction and Motivation

Various safety, economy and comfort requirements against automated vehicles pose complex decision and control challenges for research teams in the field of vehicle control design. A possible solution to the adaptation to the environment of the vehicle is to use increased number of information on the road and traffic through vehicle to vehicle (V2V) and vehicle to infrastructure (V2I) communication. The information is used in different layers of the longitudinal control in automated vehicles, such as perception, navigation, design of the route and the speed profile [1].

In the recent years several design methodologies in the field of enhanced energy efficient driving systems on several vehicle control tasks have been developed. An overview about the principles of the energy efficient cruise control has been proposed in [2]. The consideration of forthcoming terrain characteristics has been handled by using a receding horizon control in real experiments in [3]. The work of [4] has presented a deep learning-based eco-driving solution to electric vehicles, in which information about the surrounding vehicles has also been incorporated. Eco-cruise control system for automated vehicles in intersection scenarios has been implemented

in [5]. Systematic design and analysis methods for predictive cruise control systems with the consideration of road and traffic information have been presented in [6].

Due to various external information sources the achieved performance level of the automated vehicle control can depend on the quality of the communicated data [8]. The source of the information might be static datasets, e.g., terrain characteristics or speed limit rules on the road. Nevertheless, some important information can vary dynamically, such as variable speed limits on high-speed roads, traffic flow information and actual motion information of the surrounding vehicles [7]. Although these information can be important to provide energy-efficient and comfortable motion for automated vehicles, the degradations in the communicated data, and thus, a challenge is to build reliable architectures, which are less dependent on the degradation of the communicated data and thus, the predefined performances can be guaranteed.

The performances of enhanced cruise control systems can be classified based on their priorities. There are primary performance requirements in safety-critical systems, especially in cruise control systems, which must be guaranteed by the control during the entire operation of the closed-loop system. Primary performances are related to keeping safe distance, i.e. from the preceding vehicle and from the follower vehicle in the case of a lane change maneuver. Moreover, a primary performance is to keep vehicle speed in a bounded range of the speed limit, with which the violation of the speed regulations or the dangerously slow motion of the vehicle in a high-speed road can be avoided. Moreover, the performances of the cruise control systems may have another group, the secondary performances, which are requested to consider by the control system, e.g. comfort criteria, energy consumption minimization or traveling time requirements. These performances are requested to maintain due to the expectations of the users, but they can be violated in critical situations, e.g. if a collision is predicted. The presented various performance requirements demand increased number of information sources, especially communicated data.

The goal of the paper is to propose a design framework for enhanced cruise control systems, with which guarantees on the primary performances are provided. In the framework two controllers are designed. It is designed a controller based on the robust Linear Parameter-Varying (LPV) control theory, which uses on-board sensor information and limited number of external information. The controller is able to provide guaranteed primary performances together with a supervisory strategy. The minimum performance level of the enhanced cruise control on the primary performances is equivalent to the performance level of the robust LPV control on the primary performances. Furthermore, a predictive optimal cruise control is also designed, in which several external information is incorporated. The proposed predictive control system is able to maintain primary and secondary performances effectively, but the primary performances cannot be guaranteed for all scenarios. The design of the predictive cruise control is based on the method, which is presented in [6]. During the cruising of the automated vehicle both controllers compute their control signal parallel. The control intervention based on the two signals is computed by a supervisory strategy.

The enhanced cruise control for automated vehicles is composed of the robust LPV

control, the nonlinear predictive optimal control and the supervisor. Interconnection between them is created by scheduling variables and known uncertainties, which are taken part of the robust LPV control design. The motivation behind the robust LPV formalism is flexibility, which can be achieved by the adaptation capability of the controller through the selection of the scheduling variable.

The contribution of the paper is an enhanced cruise control system, which is able to solve the complex cruising problem with several performances for automated vehicles. The novelties of the proposed method are summarized as follows. First, the proposed method provides theoretical guarantees on the performance level of the primary performances. Second, the guaranteed performance level of the system is less dependent on the degradation of the communicated data from the external information sources, which can provide an improved level of safety for automated vehicles.

The paper is organized as follows. The strategy of the nonlinear predictive optimal control, which considers various information sources is presented in Section 2. The robust LPV-based framework for modeling and control design is proposed in Section 3. Section 4 proposes the supervisory strategy, and then, the design of the robust LPV controller in an iterative framework is presented in Section 5. Section 6 illustrates the effectiveness of the proposed method. Finally, the consequences of the design method are summarized in Conclusions.

## 2 Design of Predictive Cruise Control for Automated Vehicles

The role of the section is to present the design method of the predictive cruise control briefly. The aim of the description is to provide an overview about the formulation of the performances and the incorporation of the external information in the predictive control problem. A thorough discussion of the method is found in [6].

The predictive cruise control can use various information sources, i.e., in this paper four different information sources are considered to be available. First, the automated vehicle has information from topography database, which provides altitude and road curvature information. The road section ahead of the vehicle is divided into  $n$  number of segments, where the lengths of the segments are selected to have constant inclinations. Second, the vehicle has information about speed limitations on the road segments. Since speed limitations can also depend on the actual road construction works and variable speed limit signs in high-speed roads, it can require information from static road map and V2I communication. Third, information about the average traffic speed on the forthcoming road section and the state of the traffic lights expect communication with the traffic control system. Fourth, information about the actual speed and the positions of the surrounding vehicles can require V2V communication and on-board sensors, e.g. radar measurements.

The performances of the predictive cruise control are formed as follows. A primary performance of the vehicle is to keep safe distance from the preceding vehicles in the own lane and from the follower vehicles in the case of a lane change maneuver on the entire horizon. As an assumption, it is considered that the vehicles move in the

same directions on the road. Moreover, motion information about the surrounding vehicles are considered in a predefined region of interest, which leads to  $N_p$  number of preceding vehicles and  $N_f$  number of follower vehicles. Formally, it leads to the conditions

$$e^{k_p} + \sum_{i=1}^j \left( \eta_i^{k_p} - \xi_i \right) \geq d_{safe}, \quad \forall j \in \{1, \dots, n\}, \quad \forall k_p \in \{1, \dots, N_p\} \quad (1a)$$

$$e^{k_f} + \sum_{i=1}^j \left( \xi_i - \eta_i^{k_f} \right) \geq d_{safe}, \quad \forall j \in \{1, \dots, n\}, \quad \forall k_f \in \{1, \dots, N_f\} \quad (1b)$$

where  $k_p, k_f$  represent the indexes of the preceding and follower vehicles,  $e^{k_p}, e^{k_f}$  are the actual distance between vehicle  $k_p, k_f$  and the automated vehicle and  $d_{safe}$  is the requested safe distance. Index  $j$  represents the road segment and  $\sum_{i=1}^j \xi_i$  is the predicted

longitudinal displacement of the automated vehicle until step  $j$  and  $\sum_{i=1}^j \eta_i^{k_p}, \sum_{i=1}^j \eta_i^{k_f}$  are the predicted displacements of vehicle  $k_p$  and  $k_f$ . Relations in (1) represent that the predicted distance between the automated vehicle and a surrounding vehicle until horizon  $j$  cannot be smaller than the predefined safe distance. If the relations are guaranteed, the safe distances from all surrounding vehicles on the entire horizon are kept.

Further primary performance of the control is keeping vehicle speed in a limited range around reference speed  $v_{ref,i}$  in segment  $i$ .  $v_{ref,i}$  is selected based on the speed limitation, road curvature, average traffic speed [6, 9]. The performance is formed as

$$\dot{\xi}_i \in [v_{min,i}; v_{max,i}], \quad \forall i \in \{1, \dots, n\}, \quad (2)$$

where  $\dot{\xi}$  is the speed of the automated vehicle and  $v_{min,i}, v_{max,i}$  values are the limits (minimum and maximum) of the speed range, in which the vehicle speed can vary. Performance (2) guarantees keeping speed limitations. Furthermore, it guarantees the avoidance of the dangerously slow motion of the automated vehicle. The values of  $v_{min,i}, v_{max,i}$  are derived from the value of the speed reference  $v_{ref,i}$  on each segment, e.g.  $-20\%, +5\%$  related to  $v_{ref,i}$ .

One of the most important secondary performance in the cruise control problem is to achieve minimum control intervention on the road horizon ahead of the automated vehicle, which leads to the criterion

$$\sum_{i=1}^n |F_{l,i}| \rightarrow \min, \quad (3)$$

where  $F_{l,i}$  represents traction/braking force on segment  $i$  of the horizon.

Another secondary performance is to minimize traveling time of the vehicle. Since the shortest traveling time is equivalent with the maximum speed motion of the vehicle, it can be transformed to the speed objective as

$$|v_{max,i} - \dot{\xi}_i| \rightarrow \min, \quad \forall i \in \{1, \dots, n\}. \quad (4)$$

The motions of the automated vehicles can have impact on the characteristics of the traffic flow, because the speed profiles of the automated vehicles can differ from the speed profiles of the human-driven vehicles. This impact has increasing importance through the increase of the traffic density and the ratio of the automated vehicles in the traffic flow. A further secondary performance of the control is that motion of the automated vehicles must have advantageous impact on the traffic flow. It means that the output flow of the traffic network  $q_{out}$  must be maximized, such as

$$q_{out} \rightarrow \max. \quad (5)$$

The relationship between  $q_{out}$ , the speed selection strategy of the automated vehicles, the ratio of the automated vehicles and the traffic density is characterized in [6].

### Formulation of the Optimization Process

The computation of the actual control input  $F_{l,1}$  is based on a predictive optimal control strategy, which considers the previously defined performance specifications [6]. It leads to a hierarchical optimization structure. In the low level of the structure a solution to the secondary performance problem is found, while in the high level the priority performance criteria are incorporated. The interconnection between the levels is provided by a parameter  $R$ , which is interpreted below.

In the low level of the optimization, weights  $Q, \gamma_i, i \in \{1, \dots, n\}$  are defined to all the segments on the horizon. Their role is to define the importance of each segments in the design of the current speed. Weight  $Q$  determines the tracking requirement of the predefined actual reference speed  $v_{ref,0}$ , which is related to the current segment of the vehicle. The road inclinations  $\alpha_i$  and the reference speeds on the segments of the horizon ahead of the vehicle are considered through the weights  $\gamma_i$ . The result of the predictive control is a reference speed  $\lambda$  for the vehicle, which is characterized by the weights  $Q, \gamma_i$ , such as

$$\lambda = \sqrt{\vartheta - 2s_1(1-Q)(\ddot{\xi}_0 + g\sin\alpha)}, \quad (6)$$

where  $\ddot{\xi}_0$  is the longitudinal acceleration,  $s_1$  is the length of first road segment and  $\vartheta$  incorporates force and reference speed components of the forthcoming road sections:

$$\vartheta = Qv_{ref,0}^2 + \sum_{i=1}^n \gamma_i v_{ref,i}^2 + \frac{2}{m} \sum_{i=1}^n s_i F_{di,r} \sum_{j=i}^n \gamma_j, \quad (7)$$

where the known longitudinal force resistance  $F_{di,r}$  contains the road inclination in segment  $i$ .

The selection of  $Q, \gamma_i$  values are based on the secondary performance criteria. Actual control force can be expressed in a form, which depends on  $Q$  and  $\gamma_i$ . Through the transformation of (3) to a quadratic criterion  $F_{l,1}^2 \rightarrow \min$ , the following optimization problem is yielded

$$(\beta_0(\bar{Q}) + \beta_1(\bar{Q})\bar{\gamma}_1 + \dots + \beta_n(\bar{Q})\bar{\gamma}_n)^2 \rightarrow \min \quad (8)$$

with the constraints  $0 \leq \bar{Q}, \bar{\gamma}_i \leq 1$  and  $\bar{Q} + \sum \bar{\gamma}_i = 1$ .  $\bar{Q}, \bar{\gamma}_i$  are the solutions of (8) and  $\beta_0(\bar{Q}), \beta_i(\bar{Q})$  are matrices. Objective (8) is nonlinear in  $Q$ , but for a fixed  $Q$  value it leads to a quadratic optimization problem in  $\gamma_i$  with constraints. Secondary performance (4) is transformed to the minimization of the difference between the current speed and the reference speed, such as

$$|v_{ref,0} - \dot{\xi}_0| \rightarrow \min. \quad (9)$$

The solution of (9) is achieved by selecting the weights  $\check{Q} = 1$  and  $\check{\gamma}_i = 0, i \in [1, n]$ , because in this case the automated vehicle tracks the actual reference speed value. The balance between the secondary performances is created through the selection of parameter  $0 \leq R \leq R_{max} \leq 1$ , such as

$$Q = R\bar{Q} + (1 - R)\check{Q} = 1 - R(1 - \bar{Q}) \quad (10a)$$

$$\gamma_i = R\bar{\gamma}_i + (1 - R)\check{\gamma}_i = R\bar{\gamma}_i, \quad i \in \{1, \dots, n\}. \quad (10b)$$

If  $R$  is selected for a high value, the minimization of the control force of the automated vehicle is preferred. It can lead to a reduced speed for the vehicle, which considers the forthcoming road and traffic information in the computation of  $F_{l,1}$ . But, if  $R$  has a low value, the speed of the vehicle is close to  $v_{ref,0}$ , which means that minimum traveling time is preferred. Thus, the selection of  $R$  has a high impact on the balance between the performances traveling time and control force, and consequently, on the speed profile of the automated vehicle. The value of  $R_{max}$  is determined by performance (5), which is related to the maximization of the traffic flow. The actual value of  $R_{max}$ , whose selection can result in high  $q_{out}$ , depends on the actual traffic density and the ratio of the automated vehicles in the traffic. The relationship is characterized by a nonlinear function, which is based on scenario-based studies [6].

In the high level of the optimization architecture the goal is to calculate  $R$ , with which the primary performances can be considered. The purpose of the optimization is to maximize  $R$ , which leads to an energy-efficient motion with advantageous impact on the traffic flow. Nevertheless, in the high level optimization the primary performances (1)-(2) are handled as constraints of the optimization process. Thus,  $R$  must be selected as high as possible, but the resulted speed profile must guarantee primary performances. The resulted high-level optimization problem is

$$\max_{[0, R_{max}]} R \quad (11)$$

such that the constraints (1)-(2) are guaranteed. The result of the optimization on the high-level is  $R$ , which is used in the computation of  $Q, \gamma_i$ , see (10). Furthermore,  $Q, \gamma_i$  are applied in (6), which induces a speed tracking problem, whose result is the actual control force  $F_{l,1}$ . Through the values of  $\xi_i$  and  $\dot{\xi}_i$  in the constraints (1)-(2), the result of the low-level optimization has an impact on the high-level. Thus, the maximization of  $R$  is an iterative process, until the appropriate value is achieved.

The presented optimization process can provide excellent control force for the vehicle, which considers several performance requirements. However, it is difficult to verify the result of the optimization through in theory due to the following limitations of the method.

- The control strategy requires several communicated data, whose safety and security challenges have been presented in Section 1.
- The maintenance of several performances requires complex control structure, which contains a hierarchical nonlinear optimization process. Moreover, the optimization problem depends on the actual traffic scenario, e.g., the number of constraints depends on the actual number of vehicles. Thus, it is difficult to find a compact, offline solution of the optimization process, which can be examined, e.g., from the aspect of the parameter sensitivity. Instead, the method can be verified through simulations and experimental scenarios.
- Constraints (1)-(2) depend on the prediction of the preceding/follower vehicle motion. It presupposes a vehicle motion model for the vehicles in the local surroundings, whose difference from the real vehicle motion can degrade the primary performance.

Therefore, the resulted nonlinear predictive optimal control strategy cannot be used alone in the automated vehicle cruise control system. It is requested to find a control strategy, with which the primary performances can be guaranteed, while the advantages of the predictive cruise control can be preserved in most of the vehicle cruising. It leads to the concept of the enhanced cruise control, as proposed in the rest of the paper.

### 3 Architecture of the Enhanced Cruise Control System

The basic idea of the control strategy is to design a robust LPV controller and a supervisory strategy, which can modify the control input of the predictive cruise control if the primary performances are violated.

The output of the predictive cruise control is represented as

$$u_P = \mathcal{F}(y_P) \quad (12)$$

where  $u_P = F_{I1}$  denotes the control input of the predictive cruise control,  $y_P$  vector contains the inputs of the controller with  $m_P$  elements and  $\mathcal{F}$  represents the predictive cruise controller itself. Moreover, the control signal  $u_K$  is the output of a robust LPV controller, such as

$$u_K = \mathcal{K}(\rho_P, y_K) \quad (13)$$

where  $\mathcal{K}$  represents the robust LPV controller and  $y_K$  is the vector of the measured signals with  $m_K$  elements. In (13)  $\rho_P \in \rho_P$  vector contains the scheduling variable of the controller, which is derived from the following control rule.

The most important assumption of the proposed method is that the actual value of the control signal  $u$  can be expressed in a linear form of  $u_K$ . If the primary performances are not violated by  $u_P$ , then  $u = u_P$  is selected. Thus, under the consideration that the primary performances are not violated, the relationship between  $u_K$  and  $u_P$  with the conditions is formed as

$$u_P = \rho_P^* u_K + \Delta_P^*, \quad \text{if } \rho_P^* \in \rho_P, \quad \Delta_P^* \in \Lambda_P, \quad (14)$$

where  $\rho_P^*$  and  $\Delta_P^*$  are time-dependent weighting signals.  $\rho_P^* = [\rho_{P,min}; \rho_{P,max}]$ ,  $\Delta_P^* = [\Delta_{P,min}; \Delta_{P,max}]$  represent domains in (14), where  $\rho_{P,min}$ ,  $\rho_{P,max}$ ,  $\Delta_{P,min}$ ,  $\Delta_{P,max}$  are scalars. The sets of the domains are denoted by  $\rho_P$ ,  $\Lambda_P$ . In (14) the conditions are guaranteed, if the primary performances are not violated. Thus, it can be find  $\rho_P^*$ ,  $\Delta_P^*$  pair and  $u = u_P$ . But, if  $\rho_P^* \notin \rho_P$  or  $\Delta_P^* \notin \Lambda_P$ , the variables  $\rho_P^*$ ,  $\Delta_P^*$  are limited with the boundaries of  $\rho_P$  and  $\Lambda_P$  during the computation of the control signal  $u$ . In this case  $u$  can significantly differ from  $u_P$ . The previous cases lead to a control strategy, which contains all scenarios as

$$u = \rho_P u_K + \Delta_P, \quad (15)$$

where

$$\rho_P = \min \left( \max (\rho_P^*; \rho_{P,max}); \rho_{P,min} \right), \quad (16a)$$

$$\Delta_P = \min \left( \max (\Delta_P^*; \Delta_{P,min}); \Delta_{P,max} \right). \quad (16b)$$

Thus, the concept of providing guaranteed primary performances is based on the bounding of  $\rho_P, \Delta_P$ , the relations in (16) result in  $\rho_P \in \rho_P$  and  $\Delta_P \in \Lambda_P$ . Therefore, if it is possible to design a robust LPV control with the scheduling variable  $\rho_P, \Delta_P$  and the uncertainty  $\Delta_P \in \Lambda_P$ , the primary performances can be guaranteed through the appropriate selection of  $\rho_P, \Delta_P$  values. In the control architecture the supervisor is responsible for the selection of  $\rho_P, \Delta_P$  values.

The architecture of the proposed enhanced cruise control strategy is shown in Figure 1. In the control process  $u_P$  and  $u_K$  are computed simultaneously. The role of the supervisor is to select  $\rho_P, \Delta_P$  and to generate  $u$  based on the rule (15).

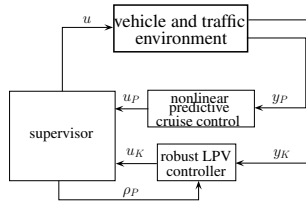


Figure 1

Scheme of the enhanced cruise control strategy

In the proposed enhanced cruise control architecture the selections of  $\rho_P, \Delta_P$  and  $\rho_P, \Lambda_P$  have high influence on the operation of the system. If the ranges of the domains are selected small,  $u_P$  is often saturated due to the limitations of domain boundaries (16). But, if the ranges  $\rho_P, \Lambda_P$  have insufficiently high values, the resulted robust LPV controller can be conservative because of the increased robustness requirements. The objective of  $\rho_P, \Delta_P, \rho_P, \Lambda_P$  selections is to provide  $u$ , with which  $u_P$  is approximated, while the primary performances are guaranteed. The objective results in the maintenance of the secondary performances, when  $u$  approximates  $u_P$ .



It might be suggested to find a joint control design and supervisor design algorithm, whose result is the selection of  $\rho_P, \Delta_P$  and  $\rho_P, \Lambda_P$  simultaneously and thus, the optimization problem

$$\min_{\rho_P, \Delta_P, \rho_P, \Lambda_P} (u - u_P)^2 \quad (17)$$

is performed. However, the design of the robust LPV control is an offline process, which requires the preliminary selection of  $\rho_P, \Lambda_P$ , while the selection of  $\rho_P, \Delta_P$  is influenced by the actual control interventions. Instead of the joint design (17) an approximation of the optimization is presented, in which the design of the robust LPV controller with the selection of  $\rho_P, \Lambda_P$  is divided from the design of the supervisor with the selection of  $\rho_P, \Delta_P$ . The objectives of both design processes are the same, i.e. the minimization of the difference between  $u$  and  $u_P$ . Although the design processes are separated, both of them influence the achieved performance level of the enhanced cruise control.

## 4 Design of the Supervisory Strategy

The purpose of the supervisor is to provide control force actuation  $u$  through the selection of  $\rho_P, \Delta_P$ , with which the primary performances during the cruising of the vehicle are guaranteed. The selection is based on the signals  $u_P, u_K$ , which are the inputs of the supervisor. The output of the supervisor  $u$  is constructed through (15), and moreover, the resulted  $\rho_P$  is used in the operation of the robust LPV control.

The design of the supervisor is based on the simplified longitudinal model of the vehicle:

$$m\ddot{\xi} = F_l - F_d, \quad (18)$$

where  $m$  is the mass of the vehicle. The state vector is  $x = [\dot{\xi} \quad \xi]^T$ , where  $\xi$  represents the longitudinal motion of the vehicle,  $w = F_d$  contains the longitudinal disturbances and  $u = F_l$  involves the longitudinal control force. The state-space representation of the system is formed as

$$\dot{x} = Ax + \hat{B}_1 w + \hat{B}_2 u, \quad (19)$$

where  $x$  represents the state vector and  $A, \hat{B}_1, \hat{B}_2$  are matrices in the representation of the system.

The state-space representation of the system is reformulated using the predefined control strategy (15), the control input of the robust LPV controller  $u_K$  is used in the expression  $u = \rho_P u_K + \Delta_P$ . Therefore, the state-space representation of the system (19) is reformulated through the relationship between  $u$  and  $u_K$  as

$$\dot{x} = Ax + B_1 w_K + B_2(\rho_P) u_K, \quad (20)$$

where the disturbance vector  $w_K$  in the state-space representation (20) is composed as  $w_K = [w \quad \Delta_P]^T$  and the matrices are  $B_1 = [\hat{B}_1 \quad B_2]$  and  $B_2(\rho_P) = \hat{B}_2 \rho_P$ . Thus, the system is transformed into a robust LPV representation.

## Specification of Conditions to Provide Guarantees on Primary Performances

The conditions to provide primary performances through the supervisor are specified based on the derived system formulation (20).

Performance (1) in the supervisor design process is focused on keeping safe distance from the closest preceding vehicle and from the closest follower vehicle of another lane, which leads to  $N_p = 1, N_f = 1$ . The goal of this simplification is to use less communicated data in the computation of  $\rho_p, \Delta_p$ . The selection of the closest vehicles is performed continuously during the operation of the supervisor based on on-board sensor measurements. If a vehicle in the region of interest of the sensors is not found (e.g., the lane of the automated is empty ahead or behind), a virtual vehicle is considered to be on the bound of the region.

The prediction of the forthcoming distance  $d^{kp}$  between the preceding vehicle and the automated vehicle is formulated based on their accelerations. The time-dependent function of  $d^{kp}$  is based on (18) as

$$\ddot{d}^{kp}(t) = \ddot{\eta}^{kp}(t) - \ddot{\xi}(t) = \ddot{\eta}^{kp}(t) - \frac{F_l(t)}{m} + \frac{F_d(t)}{m}. \quad (21)$$

Through the integration of (21) the forthcoming speed difference in time  $T$  can be derived as

$$\dot{d}^{kp}(T) = \int_0^T \ddot{d}^{kp}(t) dt = \int_0^T \left( \ddot{\eta}^{kp}(t) - \frac{F_l(t)}{m} + \frac{F_d(t)}{m} \right) dt \quad (22)$$

The integration requires knowledge about the functions  $\ddot{\eta}^{kp}(t)$  and  $F_d(t)$ . But, it can be difficult to predict the forthcoming acceleration command of the preceding vehicle and the forthcoming road disturbances. In case of a safe control strategy, these functions are substituted by constant values, which are resulted by worst-case scenarios. It is considered that  $a_{min} \leq \ddot{\eta}^{kp}(t) + \frac{F_d(t)}{m}$ , where  $a_{min}$  represents the worst case scenario, when the preceding vehicle has maximum deceleration and the road disturbance has minimum value. The value of  $a_{min}$  is a design parameter, which can be selected based on preliminary experimental results. Using  $a_{min}$ , (22) is computed as

$$\dot{d}^{kp}(T) = a_{min}T - \frac{F_l}{m}T + \dot{d}^{kp}(0) = a_{min}T - \frac{F_l}{m}T + \dot{\eta}^{kp}(0) - \dot{\xi}(0), \quad (23)$$

where  $\dot{d}^{kp}(0) = \dot{\eta}(0) - \dot{\xi}(0)$  is the speed difference at time  $t = 0$  and  $F_l(t)$  is assumed to be constant between 0 and  $T$ . The predicted distance between the vehicles is resulted by the integration of (23), such as

$$d^{kp}(T) = \frac{a_{min}T^2}{2} - \frac{F_l T^2}{2m} + \dot{\eta}^{kp}(0)T - \dot{\xi}(0)T + e^{kp}, \quad (24)$$

where  $e^{kp}$  is the measured distance between the preceding vehicle and the automated vehicle in time  $T = 0$ . The prediction in (24) requires measurement of the actual

distance  $e^{k_p}$  and the relative speed between the automated vehicle and the preceding vehicle  $\dot{\eta}^{k_p}(0) - \dot{\xi}(0)$ , which can be performed through on-board sensors, e.g., radar.

Similarly, the predicted distance between the automated vehicle and the follower vehicle  $k_f$  can be derived from the second derivative of the distance between them as  $\ddot{d}^{k_f}(t) = \ddot{\xi}(t) - \ddot{\eta}^{k_f}(t)$ . The worst-case scenario is characterized by the acceleration  $a_{max}$  through the expression  $\ddot{\eta}^{k_f}(t) + \frac{F_d(t)}{m} \leq a_{max}$ , which leads to the predicted distance

$$d^{k_f}(T) = \frac{F_l T^2}{2m} - \frac{a_{max} T^2}{2} + \dot{\xi}(0)T - \dot{\eta}^{k_f}(0)T + e^{f_p}. \quad (25)$$

The formulation of the primary performances, which means that safe distances from the preceding vehicle and the follower vehicle must be kept, are written as inequalities

$$\frac{a_{min} T^2}{2} - \frac{F_l T^2}{2m} + \dot{\eta}^{k_p}(0)T - \dot{\xi}(0)T + e^{k_p} \geq d_{safe}, \quad (26a)$$

$$\frac{F_l T^2}{2m} - \frac{a_{max} T^2}{2} + \dot{\xi}(0)T - \dot{\eta}^{k_f}(0)T + e^{f_p} \geq d_{safe}. \quad (26b)$$

Since  $u = F_l$  and  $u = \rho_P u_K + \Delta_P$  (15), the inequalities (26) are rewritten as

$$\frac{a_{min} T^2}{2} - \frac{(\rho_P u_K + \Delta_P) T^2}{2m} + \dot{\eta}^{k_p}(0)T - \dot{\xi}(0)T + e^{k_p} \geq d_{safe}, \quad (27a)$$

$$-\frac{a_{max} T^2}{2} + \frac{(\rho_P u_K + \Delta_P) T^2}{2m} + \dot{\xi}(0)T - \dot{\eta}^{k_f}(0)T + e^{f_p} \geq d_{safe}. \quad (27b)$$

Thus, it is necessary to select  $\rho_P, \Delta_P$  for given  $u_K$  to guarantee the inequalities (27), with which the primary performance of keeping safe distance is guaranteed.

Performance of keeping vehicle speed in a given speed range (2) is also based on the simplified motion model of the vehicle (18). The predicted speed of the vehicle in  $T$  is resulted through the integration of the acceleration  $\ddot{\xi}$  as

$$\dot{\xi}(T) = \int_0^T \left( \frac{F_l}{m} - \frac{F_d}{m} \right) dt. \quad (28)$$

Similarly to the derived conditions of keeping safe distance, the worst-case scenario is considered as  $|F_d| \leq F_{d,max}$ , where  $F_{d,max}$  is considered to be the upper bound of the unknown disturbance. If  $F_d > 0$ , which means that the disturbance has accelerating effect, (28) is transformed as  $\frac{F_l T}{m} + \frac{F_{d,max} T}{m} + \dot{\xi}(0)$ , where  $\dot{\xi}(0)$  is the actual speed of the automated vehicle and  $F_l$  is considered to be constant. If  $F_d < 0$ , (28) results in  $\frac{F_l T}{m} - \frac{F_{d,max} T}{m} + \dot{\xi}(0)$ , which means that  $F_d$  decelerates the vehicle. The condition for keeping vehicle speed in the given range  $[v_{min,0}; v_{max,0}]$  is formed as

$$\frac{(\rho_P u_K + \Delta_P) T}{m} + \frac{F_{d,max} T}{m} + \dot{\xi}(0) \leq v_{max,0}, \quad (29a)$$

$$\frac{(\rho_P u_K + \Delta_P) T}{m} - \frac{F_{d,max} T}{m} + \dot{\xi}(0) \geq v_{min,0}, \quad (29b)$$

in which relations  $u = F_l$  is transformed to  $\rho_P u_K + \Delta_P$  (15). Thus, it is necessary to select  $\rho_P, \Delta_P$ , with which conditions in (29) together with (27) are guaranteed.

## Optimization in the Supervisor Strategy

The selection strategy of  $\rho_P$  and  $\Delta_P$  is based on the optimization, which is presented in (17). In the supervisory process  $\rho_P, \Delta_P$  are selected during the operation of the enhanced cruise control system.

The objective of the supervisor is to provide a control input  $u$ , which is as close as possible to  $u_P$ :

$$(u - u_P)^2 \rightarrow \min. \quad (30)$$

Through (30) the control force intervention of the enhanced cruise control system approximates the output signal of the predictive cruise control. Moreover, during the selection of  $\rho_P, \Delta_P$  the criteria of (27) and (29) must be guaranteed and the constraints  $\rho_P \in \rho_P, \Delta_P \in \Lambda_P$  must also be satisfied.

The objective (30) using (15) is rearranged to a quadratic form as

$$\begin{aligned} (u - u_P)^2 &= \begin{bmatrix} \rho_P \\ \Delta_P \end{bmatrix}^T \begin{bmatrix} u_K^2 & u_K \\ u_K & 1 \end{bmatrix} \begin{bmatrix} \rho_P \\ \Delta_P \end{bmatrix} + \begin{bmatrix} -2u_P u_K \\ -2u_P \end{bmatrix}^T \begin{bmatrix} \rho_P \\ \Delta_P \end{bmatrix} + u_P^2 \\ &= \begin{bmatrix} \rho_P \\ \Delta_P \end{bmatrix}^T \beta \begin{bmatrix} \rho_P \\ \Delta_P \end{bmatrix} + \omega^T \begin{bmatrix} \rho_P \\ \Delta_P \end{bmatrix} + u_P^2, \end{aligned} \quad (31)$$

in which  $u_P^2$  is independent from  $\rho_P, \Delta_P$  and thus, it can be eliminated during the minimization process (30).

The strategy of the supervisor is to compute  $\rho_P, \Delta_P$  during the operation of the cruise control. In each step the following constrained optimization problem must be solved, which is yielded from (31) and the constraints (27), (29) together with the bounds on  $\rho_P, \Delta_P$ :

$$\min_{\rho_P, \Delta_P} \begin{bmatrix} \rho_P \\ \Delta_P \end{bmatrix}^T \beta \begin{bmatrix} \rho_P \\ \Delta_P \end{bmatrix} + \omega^T \begin{bmatrix} \rho_P \\ \Delta_P \end{bmatrix}, \quad \text{subject to} \quad (32a)$$

$$-\frac{(\rho_P u_K + \Delta_P)T^2}{2m} + \frac{a_{min}T^2}{2} + \dot{\eta}^{k_p}(0)T - \dot{\xi}(0)T + e^{k_p} \geq d_{safe}, \quad (32b)$$

$$\frac{(\rho_P u_K + \Delta_P)T^2}{2m} - \frac{a_{max}T^2}{2} + \dot{\xi}(0)T - \dot{\eta}^{k_f}(0)T + e^{f_p} \geq d_{safe}, \quad (32c)$$

$$\frac{(\rho_P u_K + \Delta_P)T}{m} + \frac{F_{d,max}T}{m} + \dot{\xi}(0) \leq v_{max,0} + S, \quad (32d)$$

$$\frac{(\rho_P u_K + \Delta_P)T}{m} - \frac{F_{d,max}T}{m} + \dot{\xi}(0) \geq v_{min,0} - S, \quad (32e)$$

$$\rho_P \in \rho_P, \quad \Delta_P \in \Lambda_P. \quad (32f)$$

In (32d)-(32e)  $S$  is a slack variable. The role of  $S$  is to set a hierarchy in the constraints and to ensure that the optimization problem returns a feasible solution [10]. For example, if the automated vehicle must be stopped to avoid the collision with a preceding vehicle and  $v_{min,0} > 0$ , the constraint (32e) cannot be guaranteed. It leads to the infeasibility of the optimization problem of (32). It must be avoided by setting

$S$  to a high value. Since the avoidance of the collision has higher priority than keeping the speed in the predefined range, the following process must be performed for the selection of  $S$ .  $S = 0$  is selected as a default value. If (32) has feasible solutions  $\rho_P, \Delta_P$ , control input  $u = \rho_P u_K + \Delta_P$  is computed. If (32) is not feasible with  $S = 0$ ,  $S$  is selected for a high value to guarantee the feasibility. Then, (32) with the new value of  $S$  is solved. The resulted  $\rho_P, \Delta_P$  are applied to provide control input  $u = \rho_P u_K + \Delta_P$ .

## 5 Design of the Robust LPV-based Cruise Control System

The aim of the robust LPV control is to provide  $u_K$  control input signal for the supervisor. The robust LPV control has importance in the situations, when the output of the predictive cruise control can violate the primary performances. Nevertheless, in most of the operation of the enhanced cruise control,  $u_P$  might be acceptable. Therefore,  $u_K$  has importance mainly in critical situations, and in these scenarios the maintenance of the secondary performances has low priority. Consequently, it is enough to use the simplified control-oriented model (18) for the robust LPV control design, with which the objective of the main functionality in cruise control, such as speed tracking can be specified as  $z_1 = v_{ref,0} - \xi$ ,  $|z_1| \rightarrow \min$ . Moreover, the minimization of the control input  $u_K$  must be considered as an objective of the robust control design:  $z_2 = u_K$ ,  $|z_2| \rightarrow \min$ . The consideration of  $u_K$  has the role to guarantee the quantification of  $z_1$  through the balance between the objectives. Furthermore, through  $z_2$  the insufficiently high longitudinal control force is avoided. The objectives  $z_1, z_2$  are composed in a vector of objectives, such as  $z_K = [z_1 \ z_2]^T$ . Using the state-space formulation of the system (20),  $z_K$  is formed as  $z_K = C_1 x + D_{11} w_K + D_{12} u_K$ , where  $w_K$  is extended as  $w_K = [F_d \ \Delta_P \ v_{ref,0}]^T$ ,  $C_1, D_{11}, D_{12}$  are matrices.

The measurement equation for the robust LPV control design is formed as  $y_K = v_{ref,0} - \xi = C_2 x + D_{21} w_K$ , where  $C_2, D_{21}$  are matrices. If  $N^p = 0$ ,  $v_{ref,0}$  is get from static map database of speed limits and the camera-based traffic sign recognition system of the vehicle. If  $N^p > 0$ , the speed information of database and the speed information of the recognition system are limited by radar measurement about  $\hat{\eta}^p$ . Thus, in the robust LPV control low number of external information is incorporated and most of the information is based on own sensors.

Finally, the plant for the robust LPV control design is formed as follows:

$$\dot{x} = Ax + B_1 w_K + B_2(\rho_P) u_K, \quad (33a)$$

$$z_K = C_1 x + D_{11} w_K + D_{12} u_K, \quad (33b)$$

$$y_K = C_2 x + D_{21} w_K, \quad (33c)$$

in which  $\rho_P$  is the scheduling variable of the system.

The control design is based on the resulted control-oriented model (33). Scaling of  $w_K$  and providing a balance between the elements of  $z_K$  require a weighting strategy in the control design method. The closed-loop interconnection structure is presented

in Figure (2). The interconnection structure contains several weighting functions. The

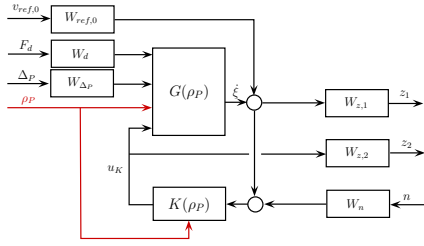


Figure 2

Closed-loop interconnection structure for robust LPV control design

weight  $W_n$  is related to the sensor characteristics on the velocity error measurement, where  $n$  represent sensor noise.  $W_d$  scales the longitudinal disturbance force  $F_d$ . The bound of  $F_d$  has also role in the supervisor design. Weight  $W_d$  is characterized as  $W_d = \frac{F_{d,max}}{T_d s + 1}$ , where  $T_d$  is a tuning parameter, which represents the dynamics of  $F_d$  variation. Similarly,  $W_{\Delta P}$  scales the uncertainty  $\Delta P$ . This weight is selected in the form of  $W_{\Delta P} = \frac{\max(|\Delta P_{min}|; |\Delta P_{max}|)}{T_{\Delta 2} s^2 + T_{\Delta 1} s + 1}$ , where  $T_{\Delta 2}, T_{\Delta 1}$  are design parameters, which represent the dynamics of the signal. The role of weight  $W_{ref,0}$  is to scale the reference signal  $v_{ref,0}$ . It is considered as a constant parameter with the supreme of  $v_{max,0}$ .

$W_{z,1}, W_{z,2}$  are the weights on the control performances, which provide a balance between them. Weight  $W_{z,1}$  has important role from the aspect of the minimum performance level of the cruise control, because it scales the tracking error  $v_{ref,0} - \dot{\xi}$ . The form of the weight is  $W_{z,1} = \frac{e_v}{T_z s + 1}$ , where  $T_z$  is a design parameter and  $e_v$  is the expected maximum tracking error. The selected form guarantees that the tracking error is  $e_v$  in steady state. The selection of  $e_v$  must guarantee that  $e_v \leq v_{max,0} - v_{ref,0}$  and  $e_v \leq v_{ref,0} - v_{min,0}$  to avoid the degradation of performance (2). Weight  $W_{z,2}$  scales the control input  $u_K$ . Its value is selected as a constant parameter, which represents the supreme of  $|u_K|$ .

The quadratic robust LPV problem is to choose the parameter-varying controller  $\mathcal{K}(\rho_P, y_K)$  in such a way that the resulting closed-loop system is quadratically stable and the induced  $\mathcal{L}_2$  norm from the disturbance  $w_K$  to the objectives  $z_K$  is less than the value  $\gamma$  [11, 12]. The minimization task is the following:

$$\inf_{\mathcal{K}(\rho_P, y_K)} \sup_{\rho_P \in \rho_P} \sup_{\substack{\|w_K\|_2 \neq 0, \\ w_K \in \mathcal{L}_2}} \frac{\|z_K\|_2}{\|w_K\|_2}. \quad (34)$$

The existence of a controller that solves the quadratic robust LPV problem can be expressed as the feasibility of a set of LMIs, which can be solved numerically. Finally, the state-space representation of the robust LPV control  $\mathcal{K}(\rho_P, y_K)$  is constructed [11, 13], which leads to the control input  $u_K$ . The input signal  $u_K$  is incorporated in the computation of  $u$  together with the selection of  $\rho_P, \Delta P$ . The control strategy results in that the minimum performance level of the closed-loop system is determined by

$\mathcal{K}(\rho_P, y_K)$ . The computation of the robust LPV controller through the Matlab tool of [17] can be efficiently performed. Moreover, in the application-oriented papers [18, 19] further details on the computation and implementation of the robust LPV control can be found.

The optimization problem (34) shows that the resulting controller depends on the domains  $\rho_P, \Lambda_P$ , which demonstrates that the selection process of  $\rho_P, \Lambda_P$  and the robust LPV design are not independent from each other. During the control design it is necessary to find a balance in the selection of the domain, which is based on an iteration process.

The goal of the iteration is to find domains  $\rho_P, \Lambda_P$ , with which  $u$  approximates  $u_P$  (17). It provides that the enhanced cruise control system operates with  $u_P$  as most as possible, without the violation of primary performances. The following optimization is based on scenarios, which are performed in each steps of the iterations:

$$\min_{\substack{\rho_{P,min}, \rho_{P,max} \\ \Delta_{P,min}, \Delta_{P,max}}} \sum_{j=1}^N (u(j) - u_P(j))^2 = \min_{\substack{\rho_{P,min}, \rho_{P,max} \\ \Delta_{P,min}, \Delta_{P,max}}} \sum_{j=1}^N (\rho_P(j)u_K(j) + \Delta_P(j) - u_P(j))^2, \quad (35)$$

where  $j$  expresses the time step and  $N$  is the length of a given scenario.

The solution of the optimization problem (35) begins with domains with high ranges, which are reduced through the following iteration process.

1. The domain of the scheduling variable  $\rho_P = [\rho_{P,min}; \rho_{P,max}]$  and the domain of the uncertainty  $\Lambda_P = [\Delta_{P,min}; \Delta_{P,max}]$  are selected high in the first step, which can result in a conservative robust LPV controller.
2. The robust LPV control with the selected domains is designed using (34).
3. The closed-loop system with the incorporation of the designed  $\mathcal{K}(\rho_P, y_K)$  and the domains  $\rho_P, \Lambda_P$  are analyzed through various scenarios. It yields in the signals  $\lambda$  and  $\xi$ , from which the cost in (35) for the scenario is calculated.
4. Due to the results of the scenarios the boundaries are modified to reduce the cost function of the optimization problem (35). The setting of the variables in the optimization can be performed through e.g., simplex search or trust region reflective methods, see [14, 15].
5. The robust LPV design, the scenarios and the evaluation (see steps 2-4) are performed until the cost (35) is higher than  $\varepsilon$ , where  $\varepsilon > 0$  is a previously selected parameter.

The results of the entire iteration process are the robust LPV controller  $\mathcal{K}(\rho_P, y_K)$  and the domains  $\rho_P, \Lambda_P$ .

## 6 Illustration of the Enhanced Cruise Control Strategy

The effectiveness of the enhanced cruise control method is demonstrated in simulation examples. Two simulations are presented, which focus on the avoidance of primary

performance degradation in various scenarios.

## 6.1 Cruising on a Congested Highway

In the first simulation example the automated vehicle travels on a section of the hilly Hungarian M1 highway, which interconnects the capital cities Budapest and Vienna. In the example there is an accident on the highway (see  $5000m$  segment point in Figure 3(a)), which results in a congestion. The traffic control system provides information about the reduction of the traffic speed between  $3500m - 5000m$ , see Figure 3(a).

The automated vehicle incorporates the traffic speed information in its enhanced cruise control strategy through  $v_{ref,i}$  (see Section 2). Since the automated vehicle has  $1000m$  prediction horizon in the example, the information about the reduced traffic speed is considered from  $2500m$ . It results in the reduction of the vehicle speed (see Figure 3(b)), with which an energy-efficient motion can be achieved through the approaching to the accident [7]. Moreover, there is a preceding vehicle ahead of the automated vehicle, which stops at  $3800m$ , when the congestion is reached, see its speed profile in Figure 3(b). The goal of the enhanced cruise control is to provide minimum control force in the cruising, while the safe distance  $d_{safe} = 20m$  from the preceding vehicle is guaranteed, especially at the stop of the preceding vehicle. The distance between the vehicles is illustrated in Figure 3(c). It can be seen that the safety distance  $20m$  is guaranteed in the given example. The control signal  $u$  and the values of  $\rho_P, \Delta_P$  are illustrated in Figure 3(d)-(f). At the end of the simulation, when the distance is reduced,  $\rho_P$  is set to zero and  $\Delta_P$  is also reduced. It results in the tracking of the preceding vehicle speed (close to zero) through the control input of the robust LPV control.

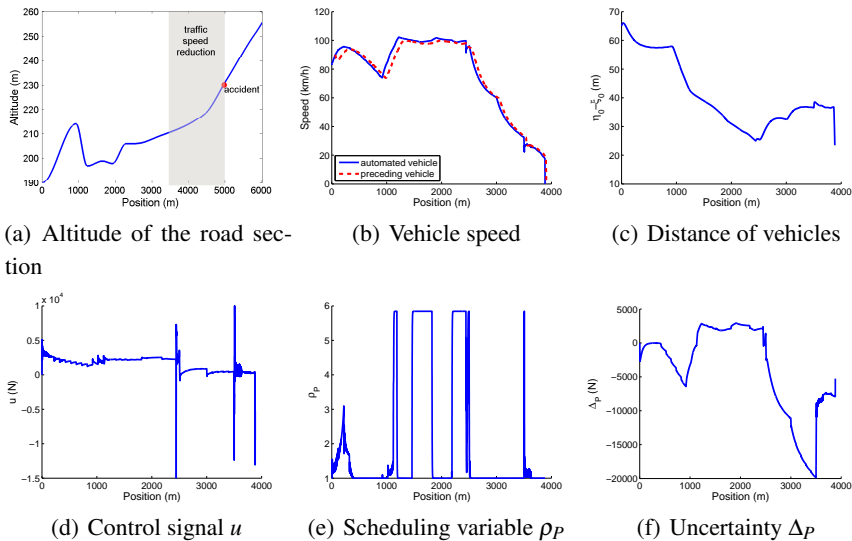


Figure 3  
Simulations of lane change scenario



## 6.2 Overtaking Scenario with Degradation in the Communication

The second simulation example presents a lane change scenario, in which the vehicle in the inner lane of a two-lane road overtakes a slower vehicle. There is also a preceding vehicle in the inner lane, which has higher speed, compared to the automated vehicle. In this situation the automated vehicle cannot change lane due to the overtaken vehicle, which is in the outer lane. Moreover, the vehicles in the inner lane also cannot be forced to reduce their speed, which means that the automated vehicle must be accelerated. The goal of the cruise control is to minimize the control force of the automated vehicle, while the safe distance between the vehicles is guaranteed.

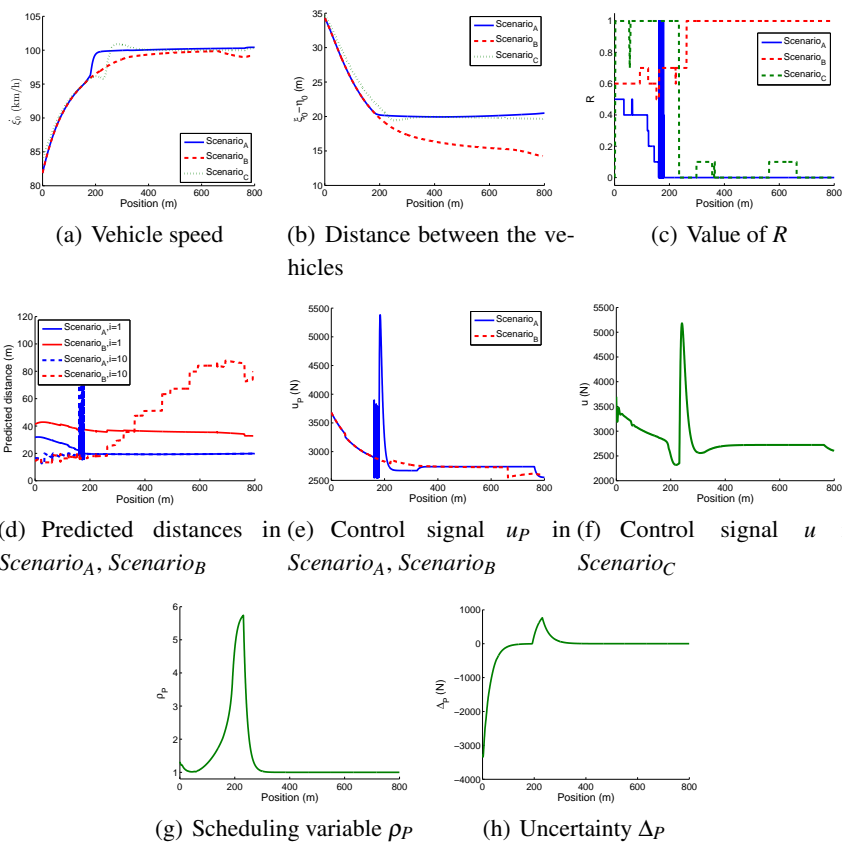


Figure 4  
Simulations in overtaking scenario

In the example three scenarios are illustrated. In all scenarios the automated vehicle has information about the longitudinal acceleration, the speed and the position of the preceding vehicle through V2V communication, which is used in the predicted cruise control system to compute  $R$ , see (11). In  $Scenario_A$  the time delay related to

the communication is  $0.05s$ , which is considered to be the nominal time delay value, while in *Scenario<sub>B</sub>* and in *Scenario<sub>C</sub>* the V2V communication has a degradation in the time delay, which is increased to  $0.5s$ . In *Scenario<sub>A</sub>* and in *Scenario<sub>B</sub>* the automated vehicle uses the presented predictive cruise control ( $u \equiv u_P$ ), while in *Scenario<sub>C</sub>* the enhanced cruise control structure is in the loop, which also uses onboard distance measurement about the distance between the vehicles. The purpose of the simulation examples is to illustrate that the proposed enhanced cruise control method is able to guarantee the safe distance, even if the V2V communication delay is degraded.

Figure 4(a) shows vehicle speed and Figure 4(b) illustrates the distance between the vehicles in each scenarios. In *Scenario<sub>A</sub>* the predictive cruise control is able to guarantee the safe distance  $20m$ , which is resulted by the increase of its speed to  $100km/h$ . The increase of the speed is resulted by the reduction of  $R$  (Figure 4(c)), which is computed based on the reduction of the predicted distances, see e.g., section  $0 \dots 200m$  of *Scenario<sub>A</sub>* in Figure 4(d). It induces sharp increase in  $u_P$ , see Figure 4(e). Thus, the predicted cruise control is able to guarantee the safe distance, if the signals in the communication have low time delay value.

If time delay is increased, the predictions of the distances in *Scenario<sub>B</sub>* significantly differ from the predictions in *Scenario<sub>A</sub>*, see Figure 4(d). Due to the increased time delay the preceding vehicle is predicted to have significantly smaller acceleration, which means that the automated vehicle focuses on the minimization of the control force. The increased  $R$  (Figure 4(c)) leads to reduced  $u_P$  (Figure 4(e)), which results in reduced speed profile (Figure 4(a)). Consequently, the safe distance between the vehicles is not kept (Figure 4(b)), which can force the preceding vehicle to unwanted braking intervention.

The resulted speed profile in *Scenario<sub>C</sub>* is illustrated in Figure 4(a). Since the supervisor uses the onboard measurement about the distance between the vehicles, the reduction in  $\xi_0 - \eta_0$  is perceived. It leads to the reduction of  $\rho_P$  and  $\Delta_P$ , with which the tracking of  $v_{ref,0}$  is highlighted. The resulted control signal  $u$  of *Scenario<sub>C</sub>* (Figure 4(f)) is close to the  $u_P$  of *Scenario<sub>A</sub>*, which results in keeping safe distance (Figure 4(b)). Thus, the enhanced cruise control system is able to guarantee safe distance, even if the time delay in the communication is significantly increased.

## Conclusions

The proposed enhanced cruise control strategy is able to provide guarantees on the specified primary performances for automated vehicles. The consequence of the proposed method is that in most of the cruise control operation, requirements against the secondary performances (e.g., energy-efficient motion of the automated vehicle) can be maintained, while the primary performances are guaranteed in the entire operation of the control. The effectiveness of the control strategy is illustrated by simulation scenarios.

The proposed enhanced cruise control strategy is independent from the internal structure of the predictive optimal cruise control. Therefore, the future challenge of the method is its application to provide guarantees for further cruise control algorithms, e.g., learning-based cruise control methods.

## Acknowledgement

The research was supported by the European Union within the framework of the National Laboratory for Autonomous Systems (RRF-2.3.1-21-2022-00002). The research was also supported by the National Research, Development and Innovation Office (NKFIH) under OTKA Grant Agreement No. K 135512.

## References

- [1] A. Sciarretta and A. Vahidi, *Energy-Efficient Driving of Road Vehicles*. Springer Verlag, 2019.
- [2] J. Han, A. Vahidi, and A. Sciarretta, “Fundamentals of energy efficient driving for combustion engine and electric vehicles: An optimal control perspective,” *Automatica*, vol. 103, pp. 558 – 572, 2019.
- [3] E. Hellström, M. Ivarsson, J. Åslund, and L. Nielsen, “Look-ahead control for heavy trucks to minimize trip time and fuel consumption,” *Control Eng. Practice*, vol. 17, no. 2, pp. 245–254, 2009.
- [4] G. Wu, F. Ye, P. Hao, D. Esaid, K. Boriboonsomsin, and M. Barth, “Deep learning-based eco-driving system for battery electric vehicles,” 2019.
- [5] M. H. Almannaa, H. Chen, H. A. Rakha, A. Loulizi, and I. El-Shawarby, “Field implementation and testing of an automated eco-cooperative adaptive cruise control system in the vicinity of signalized intersections,” *Transp. Research Part D: Transport and Environment*, vol. 67, pp. 244 – 262, 2019.
- [6] P. Gáspár and B. Németh, *Predictive Cruise Control for Road Vehicles Using Road and Traffic Information*. Springer Verlag, 2019.
- [7] B. Németh and P. Gáspár, “The relationship between the traffic flow and the look-ahead cruise control,” *IEEE Transactions on Intelligent Transportation Systems*, vol. 18, no. 5, pp. 1154–1164, May 2017.
- [8] Z. Wang, Y. Bian, S. E. Shladover, G. Wu, S. E. Li, and M. J. Barth, “A survey on cooperative longitudinal motion control of multiple connected and automated vehicles,” *IEEE Intelligent Transportation Systems Magazine*, vol. 12, no. 1, pp. 4–24, Spring 2020.
- [9] A. Mihály, B. Németh, and P. Gáspár, “Look-ahead control of road vehicles for safety and economy purposes,” *Control Conference (ECC), 2014 European*, pp. 714–719, 2014.
- [10] S. M. Thornton and S. Pan and S. M. Erlien, and J. C. Gerdes, “Incorporating ethical considerations into automated vehicle control,” *IEEE Transactions on Intelligent Transportation Systems*, vol. 18, no. 6, pp. 1429–1439, June 2017.
- [11] F. Wu, X. Yang, A. Packard, and G. Becker, “Induced  $L_2$  norm controller for LPV systems with bounded parameter variation rates,” *Journal of Robust and Nonlinear Control*, vol. 6, pp. 983–988, 1996.
- [12] C. Briat, *Linear Parameter-Varying and Time-Delay Systems*, ser. Advances in Delays and Dynamics. Springer-Verlag Berlin, 2015.

- [13] O. Sename, P. Gáspár, and J. Bokor, *Robust Control and Linear Parameter Varying Approaches*. Springer Verlag, Berlin, 2013.
- [14] J. C. Lagarias, J. A. Reeds, M. H. Wright, and P. E. Wright, “Convergence properties of the nelder-mead simplex method in low dimensions,” *SIAM Journal of Optimization*, vol. 9, no. 1, pp. 112 – 147, 1998.
- [15] T. Coleman and Y. Li, “An interior, trust region approach for nonlinear minimization subject to bounds,” *SIAM J. on Optimization*, vol. 6, pp. 418–445, 1996.
- [16] B. Németh and P. Gáspár, “Robust look-ahead cruise control design based on the  $\mathcal{H}_\infty$  method,” *IFAC-PapersOnLine*, vol. 48, no. 14, pp. 19 – 24, 2015, 8th IFAC Symposium on Robust Control Design ROCOND 2015.
- [17] A. Hjartarson and P. Seiler and A. Packard, ”LPVTools: A Toolbox for Modeling, Analysis, and Synthesis of Parameter Varying Control Systems,” *IFAC-PapersOnLine*, vol. 48, no. 26, pp. 139-145, 2015.
- [18] B. Németh, P. Gáspár, ”LPV Design for the Control of Heterogeneous Traffic Flow with Autonomous Vehicles,” *Acta Polytechnica Hungarica*, vol. 16, no. 7, pp. 233 – 246, 2019.
- [19] G. Eigner, “Novel LPV-based control approach for nonlinear physiological systems,” *Acta Polytechnica Hungarica*, vol. 14, no. 1, pp. 45–61, 2017.